Electronic structures and optical properties of butyl-passivated Si nanoparticles

Tanaka, Akinori
Saito, Ryo
Kamikake, Tadafumi
Imamura, Masaki
Yasuda, Hidehiro

(Citation)
Solid State Communications,140(7-8):400-403

(Issue Date)
2006-11

(Resource Type)
journal article

(Version)
Accepted Manuscript

(URL)
https://hdl.handle.net/20.500.14094/90000182

Electronic structures and optical properties of butyl-passivated Si nanoparticles

Akinori Tanaka [a, b *], Ryo Saito [a **], Tadafumi Kamikake [a], Masaki Imamura [b], and Hidehiro Yasuda [a, b]

[a] *Department of Mechanical Engineering, Kobe University, Nada-ku, Kobe 657-8501, Japan*

[b] *Department of Mechanical and Systems Engineering, Kobe University, Nada-ku, Kobe 657-8501, Japan*

(Received)

We have carried out the various spectroscopic studies of *n*-butyl-passivated Si nanoparticles synthesized by solution routes. Photoluminescence (PL) spectrum of *n*-butyl-passivated Si nanoparticle with mean diameter less than about 2 nm exhibits a strong emission around 3.3 eV photon energy. PL excitation (PLE) spectrum exhibits a distinct resonance around 4 eV in photon energy. Furthermore, we have carried out the valence-band photoemission measurements using a synchrotron radiation in order to directly investigate their electronic structures in the vicinity of Fermi level. From these results, the detailed optical properties and electronic structures of *n*-butyl-passivated Si nanoparticles are discussed.

PACS codes: 73.22.-f, 78.67.-n

Keywords: A. nanostructures, A. semiconductors, B. chemical synthesis, D. optical properties, E. luminescence, E. photoelectron spectroscopies, E. synchrotron radiation

* Author to whom correspondence should be addressed.
E-mail: a-tanaka@mech.kobe-u.ac.jp, Fax: +81-78-803-6123

** On leave from Department of Physics, Tohoku University, Aoba-ku, Sendai 980-8578, Japan

1. Introduction

Semiconductor nanostructures are attracting much interest from the viewpoints of both device and fundamental physics, because they show the distinctive physical and chemical properties found in neither bulk nor molecular/atomic systems. For example, zero-dimensional confinement effects on electron-hole systems (quantum confinement effect) become predominant in a semiconductor nanoparticle with a size range of a few nanometers to several tens of nanometers. Recently, the various Si nanostructures have a great interest, since it has been reported that they show a strong photoluminescence (PL) [1] and therefore there is a possibility of future integrating electronic devices with optical sensing technique. To date, numerous researches focused on the optical properties of Si nanoparticles prepared by the various methods such as chemical etching [2], ion sputtering [3], chemical vapor deposition [4], ion implantation [5], laser ablation [6], and inverse micelle method [7], *etc.* have been reported. However, these optical properties depend on the samples in the literatures and are ascribed to various sources such as quantum confinement, oxide-related species, surface state, molecular species, or impurities, *etc* [8]. Therefore, the interplay between the intrinsic quantum confinement effects and extrinsic surface/interface properties is still controversial. It is considered that the reason why the discussions regarding their optical properties are still unclear is that most of the previous works have concentrated on only their optical spectra and indirectly discussed their electronic structures from the results of optical spectroscopic measurements. In order to understand the intrinsic properties of these Si-based nanostructured materials, it is indispensable to prepare the well-defined samples and directly characterize their intrinsic electronic structures.

In this work, we have synthesized *n*-butyl-passivated Si nanoparticles with well crystalline nature and well surface-passivated surface by solution routes [9], and have performed the various spectroscopic studies. Photoemission spectroscopy has been used to directly investigate the electronic structure, but to our knowledge there is no report which highlights the electronic structures of surface-passivated Si nanoparticles. In this paper, we have directly characterized the electronic structures in the vicinity of Fermi level of alkyl-passivated Si nanoparticles by means of photoelectron spectroscopy using synchrotron radiation in addition to usual optical spectroscopic measurements. From these results, we will discuss the correlation between their optical properties and electronic structures of surface-passivated Si nanoparticles.

2. Experiment

The *n*-butyl-passivated Si nanoparticles used in this work were synthesized by the oxidation of magnesium silicide (Mg_2Si) with bromine and the subsequent passivation of Si_mBr product (Br-capped Si nanoparticle) with use of an alkyllithium reagent. Bromine and magnesium silicide were added to degassed octane. After stirring for 2 hours, this mixture was refluxed for 60 hours, and then the solvent and remaining Br_2 were removed under reduced pressure. After that, *n*-butyllithium (*n*-C_4H_9Li) was added and stirred at room temperature for 2 days, and then the solvent was evaporated in a rotary evaporator. Then, an aqueous solution of hydrochloric acid was added to dissolve and remove any salts. After hexane was added, this mixture was transferred to a separatory funnel and then was washed three times with water. Finally, the hexane phase containing the Si nanoparticle was corrected. In this work, a size-selective ultrafiltration treatment for the above crude samples was performed in order to improve the nanoparticle size distribution. The size distributions in diameter of the synthesized *n*-butyl-passivated Si nanoparticles were characterized by *ex-situ* observations with a H-7000 (Hitachi Co.) transmission electron microscope (TEM). The samples for TEM observations were prepared by drying the hexane dispersions of *n*-butyl-passivated Si nanoparticles on the amorphous carbon-coated copper TEM grids. As a further characterization, Fourier transform infrared (FTIR) spectra were measured using the NEXUS-470 (Nicolet Co.) spectrometer.

PL and PL excitation (PLE) spectra of thus synthesized *n*-butyl-passivated Si nanoparticles were measured at room temperature using RF-5300PC (Shimazu Co.) spectrometer. Synchrotron-radiation photoemission measurements were carried out using A-1 (MBS-Toyama Co.) photoelectron spectrometer at BL-5U of UVSOR-II Facility, Institute for Molecular Science, Okazaki, Japan. For the photoemission measurements, the synthesized *n*-butyl-passivated Si nanoparticles were supported on the highly oriented pyrolytic graphite (HOPG) substrates by evaporating the solvent (hexane) from the dispersion of *n*-butyl-passivated Si nanoparticles on the single-crystalline HOPG cleaved surface in a nitrogen-filled glove bag directly connected to the ultrahigh-vacuum photoelectron spectrometer. Then the samples were transferred into the photoemission analysis chamber without exposure to air. Photoemission measurements were performed with the incident photon energy of 184 eV at room temperature. The thus-prepared samples show no siginals from the contaminants. The photoemission spectra showed no change in the course of the measurements.

3. Results and Discussion

In this work, we carried out the size-selective ultrafiltration treatment for synthesized *n*-butyl-passivated Si nanoparticles in order to improve the size distribution as described above. Figures 1(a) and (b) shows the TEM micrographs of as-synthesized *n*-butyl-passivated Si nanoparticles and *n*-butyl-passivated Si nanoparticle sample after ultrafiltration treatment, respectively. As shown in Figs. 1(a) and (b), each *n*-butyl-passivated Si nanoparticle is well separated from its neighboring nanoparticles, indicating that the present Si nanoparticles are well surface-passivated by the butyl molecules. Furthermore, as shown in inset of Fig. 1(a), high-resolution TEM micrograph of present *n*-butyl-passivated Si nanoparticle shows the identical lattice fringes to bulk Si crystallite, indicative of well crystalline nature. While as-synthesized sample have a large size distribution as shown in Fig. 1(a), it is found that Si nanoparticles with diameter above 3 nm are removed after size-selective treatment by mean of ultrafiltration as shown in Fig. 1(b). While it is difficult to clearly resolve the small Si nanoparticles with diameter less than 1 nm in the present TEM observations and it is difficult to determine the exact mean diameter, a mean diameter of the sample after ultrafiltration treatment has been estimated to be less than about 2 nm from the TEM micrograph of Fig. 1(b). Figure 1(c) shows the FTIR spectrum of *n*-butyl-passivated Si nanoparticles after ultrafiltration treatment. From the literature [10], the spectral features around 2870-2960 cm^{-1} wavenumbers originate from methylene and terminated methyl (-C-CH_3, Si-CH_3 terminal –CH_3 group, and/or -C-CH_2-) stretching modes, and those around 1360-1460 cm^{-1} wavenumbers originate from methylene and terminated methyl deformation and/or scissor modes. These vibration modes are attributed to the surface passivants of alkyl chains. An important point to note is that no spectral features around 1000-1100 cm^{-1} wavenumber, attributed to Si-O stretching modes, has been observed. This indicates no oxygen contamination on the surface of the Si nanoparticle and no Si-O containing impurity in the Si nanoparticle. From these results of FTIR measurements, it is confirmed that the present Si nanoparticles are perfectly surface-passivated by *n*-butyl molecules and have no surface contamination and impurity.

Figure 2 shows PL and the corresponding PLE spectra at room temperature of *n*-butyl-passivated Si nanoparticle after ultrafiltration treatment with mean diameter less than about 2 nm. As shown in Fig. 2, PL spectra of the present Si nanoparticles exhibit the distinct emission around 3.3 eV in photon energy and no emission in the photon energy region below 2 eV. Moreover, the monotonic shifts of these emissions as a function of excitation photon energy are observed. The corresponding PLE spectra of the present Si nanoparticles exhibit

the distinct resonance around 4 eV photon energy, and the monotonic shifts of these resonances as a function of emission photon energy are also observed. It is found that these resonance energies in the PLE spectra are greater than the bulk Si band gap energy. Though there is a possibility of the luminescence from the surface-passivant molecules and/or trap states in the Si nanoparticle, PL derived from the surface-passivant molecules and/or trap states will show no excitation photon energy dependence. However, as described above, the present PL spectra show the distinct excitation photon energy dependence, and PLE spectra also show the corresponding emission energy dependence. Therefore, it is considered that the blue PL form the present *n*-butyl-passivated Si nanoparticles does not originate from the surface-passivant molecules and/or trap states such as oxide and/or defect/impurity sites. Another possibility of the origin of the present PL is considered to be result from the quantum confinement effect in the Si nanoparticle. If the quantum confinement effect is revealed in the present *n*-butyl-passivated Si nanoparticle, the energy gap (HOMO-LUMO gap) will depend on the nanoparticle size. As shown in Fig. 1(b), even sample after size-selective ultrafiltration treatment have a finite size distribution. Therefore, it is considered that the monotonic shift of PL of the present sample as a function of excitation photon energy originates from the excitation of Si nanoparticles with different sizes which have different optical transition energies. That is, the present PL observed for *n*-butyl-passivated Si nanoparticles is considered to originate from electron-hole pair recombination between the modified conduction-band (LUMO) and valence-band (HOMO) due to the quantum size effect.

In order to confirm the above discussions, we have performed the synchrotron-radiation photoemission study of the present *n*-butyl-passivated Si nanoparticle in order to directly investigate their electronic structures in the vicinity of Fermi level. Figure 3 shows the synchrotron-radiation valence-band photoemission spectrum of the present *n*-butyl-passivated Si nanoparticle with mean diameter less than about 2 nm on the HOPG substrate at room temperature with photon energy of 184 eV. Previously, the photoemission spectrum of methyl-terminated Si(111) surface and comparison with calculated density of states by DV-Xα method have reported by Miyadera *et al*. [11] From the analogy with the results of methyl-terminated Si(111) surface, the spectral features in the photoemission spectrum around 7 and 5.5 eV in binding energies originate from the C 2*p* derived states. It is considered that the spectral feature around 7 eV binding energy originate from the C-H bonds in the butyl surface-passivants, and that around 5.5 eV binding energy originate from the $\sigma_{Si\text{-}C}$ bonds between the Si nanoparticle and butyl surface-passivants. This distinct spectral feature around 5.5 eV binding energy indicates again that the present Si nanoparticles are well surface-passivated by butyl molecules. The spectral features around 3.5, 9, and 11.5 eV in

binding energies originate from the Si 3*s*- and 3*p*-derived electronic states. The additional feature around 13.5 eV in binding energy corresponds to that from HOPG substrate, since there is an uncovered region of Si nanoparticles on the HOPG substrate in the present measurement. In the inset of Fig. 3, we plot the photoemission spectrum in the vicinity of Fermi level on an expanded energy scale. In this energy region in the vicinity of Fermi level, the spectral intensity from the HOPG substrate, which reflects the vanishing semimetallic density of states toward the Fermi level, also contributes to the photoemission spectrum. As shown in inset of Fig. 3, the additional spectral intensity can be observed on the photoemission intensity from HOPG substrate. Since the contribution of C 2*s*- and 2*p*-derived states from butyl molecular orbitals do not appear in this energy region, this additional intensity in the vicinity of Fermi level is considered to originate from the valence-band structure of the present *n*-butyl-passivated Si nanoparticles. From this photoemission spectrum in the vicinity of Fermi level, we have estimated the valence-band maximum (HOMO) energy from an intersection point of two lines extrapolated by the least squares method of spectral tail of the valence-band structure of Si nanoparticles and the background signal from the HOPG substrate. From this analysis, we obtain the valence-band maximum of about 2 eV below the Fermi level. If the Fermi level is considered to be located in the middle of energy gap, the energy gap (HOMO-LUMO gap) of the present *n*-butyl-passivated Si nanoparticles with mean diameter less than about 2 nm can be estimated to about 4 eV. This value corresponds to the resonance energies in the present PLE spectra fairly well. Therefore, it is confirmed that the PL from the present *n*-butyl-passivated Si nanoparticles originate from the electron-hole pair recombination between the modified conduction-band (LUMO) and valence-band (HOMO) due to the quantum size effect. Puzder *et al*. [12] have reported the surface chemical-state dependence of the electronic structures of hydrogen-passivated Si nanoparticles by means of quantum Monte Carlo calculations. They have shown that significant changes in the HOMO-LUMO gap of fully hydrogen-passivated Si nanoparticles when the surface contains passivants other than hydrogen, in particular atomic oxygen. For example, HOMO-LUMO gap of fully hydrogen-passivated Si nanoparticle with relevant size regime to the present Si nanoparticle is about 4 eV, but that of Si nanoparticle with multiple oxygen contamination is reduced to about 2 eV. In fact, even alkyl-passivated Si nanoparticles show that the oxygen contamination induces the red shift of PL [9]. Moreover, Reboredo *et al*. [13] have recently reported the results of *ab initio* calculations using density functional theory for the various surface-passivated Si nanoparticles. They have calculated the surface-passivant dependence of HOMO-LUMO gaps of surface-passivated Si nanoparticles, and have concluded small change as a function of surface passivation, in particular when the

Si-H bond (that is, hydrogen-passivated Si nanoparticle) is replaced by a Si-C bond (that is, alkyl-passivated Si nanoparticle). These theoretical results for surface-passivated Si nanoparticles without oxygen contamination agree well with the resonance energy in the present PLE spectra and photoemission spectrum in the vicinity of Fermi level of the present *n*-butyl-passivated Si nanoparticles. Therefore, it is concluded that the present PL from perfectly n-butyl-passivated Si nanoparticles originates from the intrinsic quantum size effect and the modified electronic structure due to the intrinsic quantum confinement effect is directly confirmed by the present photoemission spectrum in the vicinity of Fermi level.

4. Summary

We have synthesized the *n*-butyl-passivated Si nanoparticles with crystalline nature and well *n*-butyl-passivated surface by the solution routes, and have performed the various spectroscopic studies. It is found that PL spectrum of *n*-butyl-passivated Si nanoparticle with mean diameter less than about 2 nm exhibits a strong emission around 3.3 eV in photon energy, and PLE spectrum exhibits a distinct resonance around 4 eV in photon energy. Furthermore, monotonic shifts of PL as a function of excitation energy and the corresponding PLE as a function of emission energy were observed. From the synchrotron-radiation photoemission spectrum in the vicinity of Fermi level, the detailed valence-band structure of the present *n*-butyl-passivated Si nanoparticle is clarified, and the valence-band maximum (HOMO) energy was estimated to about 2 eV below the Fermi level. From the comparison of optical spectra (PL and PLE spectra) and photoemission spectrum in the vicinity of Fermi level, it is concluded that the present PL originates from the electron-hole pair recombination between the modified conduction-band (LUMO) and valence-band (HOMO) due to the intrinsic quantum size effect.

Acknowledgment

This work was supported by Grant-in-Aids from the Ministry of Education, Culture, Sports, Science and Technology of Japan. This work was also supported by the grant from Hyogo Science and Technology Association. Synchrotron-radiation experiment was performed under the Joint Studies Program (2004 and 2005) of the Institute for Molecular Science. We thank T. Ito, S. Kimura, and the staffs of UVSOR-II Facility, Institute for Molecular Science, for their technical support. We also thank S. M. Kauzlarich and K. A. Pettigrew of Department of Chemistry, University of California, Davis, and T. Uchino of

Department of Chemistry, Kobe University for useful discussions.

References

[1] For example, L. T. Canham, Appl. Phys. Lett. **57** (1990) 1046.

[2] M. Neyfeh, N. Barry, J. Therrine, O. Akcakir, E. Gratton, and G. Bourianoff, Appl. Phys. Lett. **78** (2001) 1131.

[3] R. Gago, L. Vazquez, R. Cuerno, M. Varela, C. Ballesteros, and J. M. Albella, Appl. Phys. Lett. **78** (2001) 4028.

[4] X. Wu, A. Bek, A. M. Bittner, Ch. Eggs, Ch. Ossadnik, and S. Veprek, Thin Solid Film, **425** (2003) 175.

[5] Y. Q. Wang, R. Smirani, G. G. Ross, and F. Schiettekatte, Phys. Rev. B **71** (2005) 161310.

[6] X. G. Li, Y. Q. He, and M. T. Swihart, Langmuir **20** (2004) 4720.

[7] J. P. Wilcoxon, G. A. Samara, P. N. Provencio, Phys. Rev. B **60** (1999) 2704.

[8] *For example*, A. G. Cullis, L. T. Canham, and P. D. Calcott, *J. Appl. Phys.*, **82** (1997) 909.

[9] K. A. Pettigrew, Q. Liu, P. P. Power, and S. M. Kauzlarich, Chem. Mater. **15** (2003) 4005.

[10] C.-S. Yang, R. A. Bley, S. M. Kauzlarich, H. W. H. Lee, and G. R. Delgado, J. Am. Chem. Soc. **121** (1999) 5191.

[11] T. Miyadera, A. Koma, and T. Shimada, Surf. Sci. **526** (2003) 177.

[12] A. Puzder, A. J. Williamson, J. C. Grossman, and Griulia, Phys. Rev. Lett. **88** (2002) 097401.

[13] F. A. Reboredo and G. Galli, J. Phys. Chem. B **109** (2005) 1072.

.

Figure Captions

Fig. 1. (a) TEM micrographs of as-synthesized *n*-butyl-passivated Si nanoparticles. The inset shows the high-resolution TEM micrograph. (b) TEM micrographs of *n*-butyl-passivated Si nanoparticle after size-selective ultrafiltration treatment. (c) FTIR spectrum of *n*-butyl-passivated Si nanoparticles after ultrafiltration treatment.

Fig. 2. PL and PLE spectra of *n*-butyl-passivated Si nanoparticle after ultrafiltration treatment with mean diameter less than about 2 nm. Excitation photon energies for PL measurements are indicated on each PL spectrum. Observed PL photon energies for PLE measurements are also indicated on each PLE spectrum.

Fig. 3. Valence-band photoemission spectrum of *n*-butyl-passivated Si nanoparticles with mean diameter less than about 2 nm supported on the HOPG substrate at room temperature measured with photon energy of 184 eV using synchrotron radiation. The inset shows the photoemission spectrum in the vicinity of Fermi level.

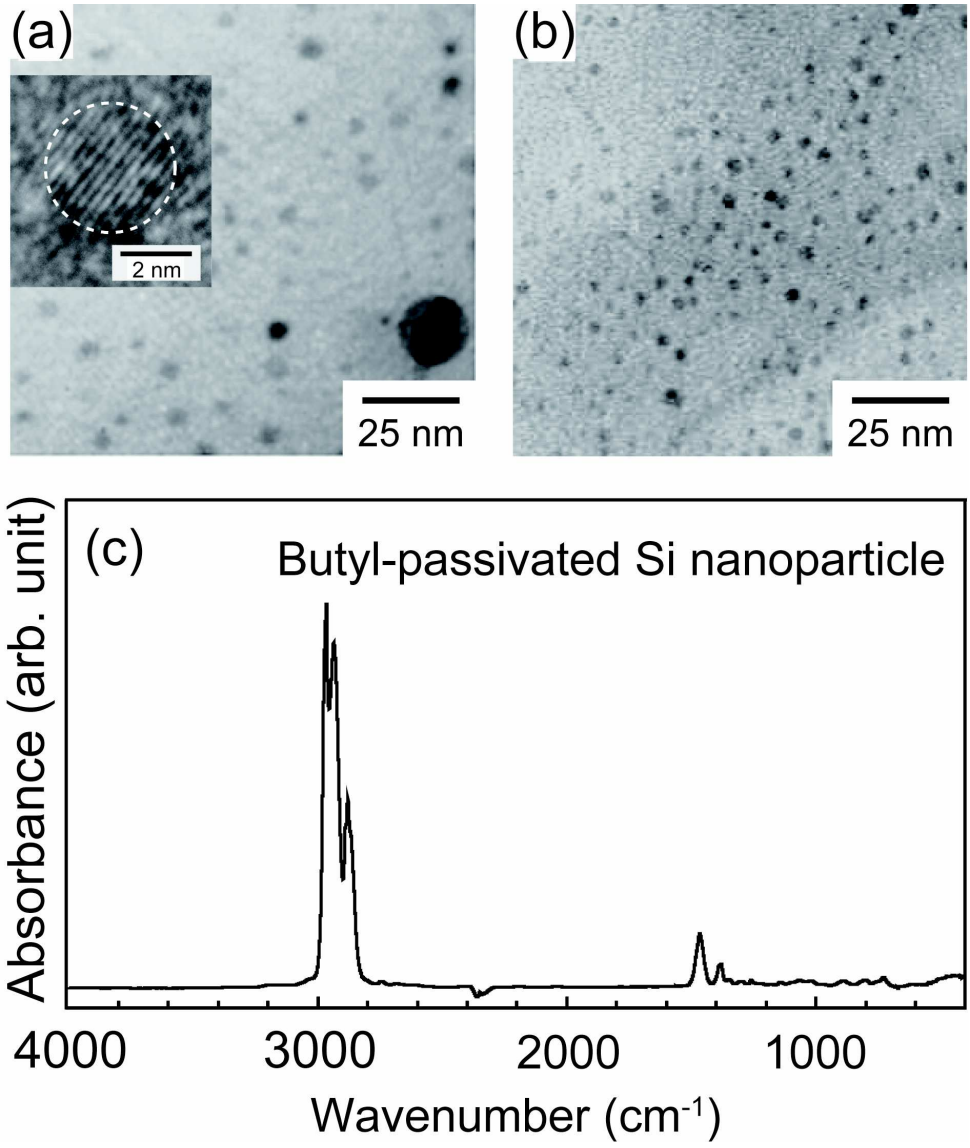

Fig. 1.

A. Tanaka *et al*.

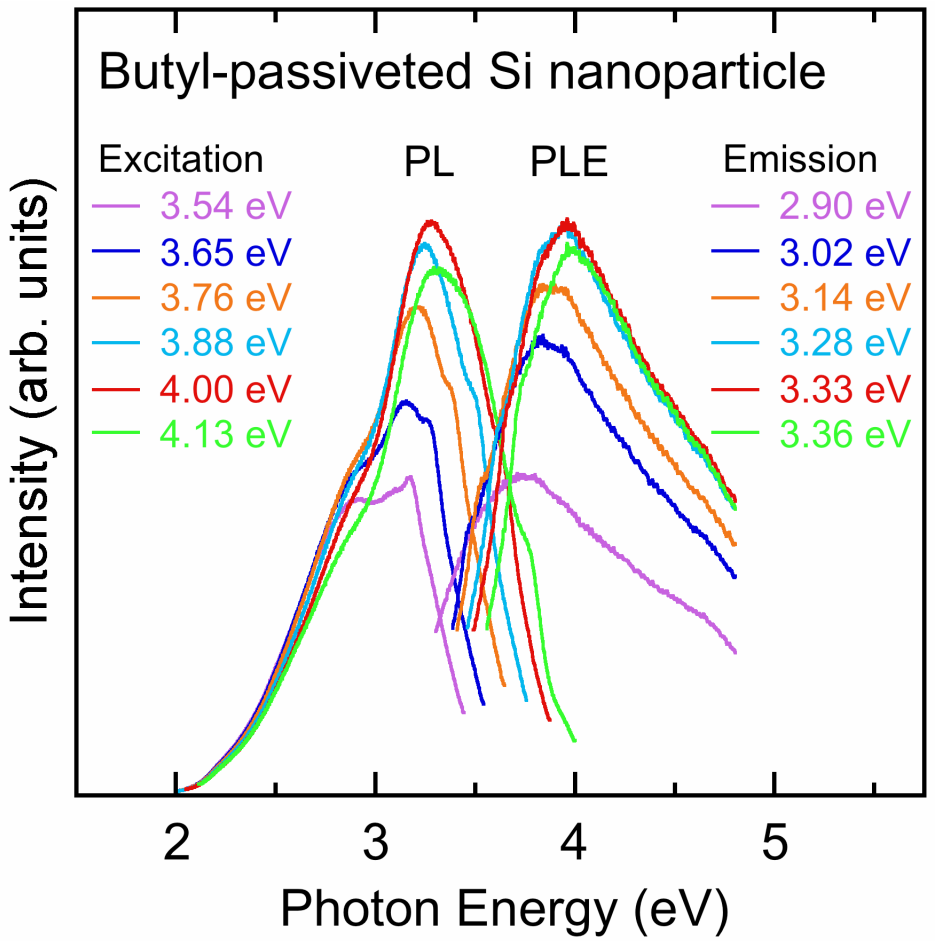

Fig. 2.

A. Tanaka *et al*.

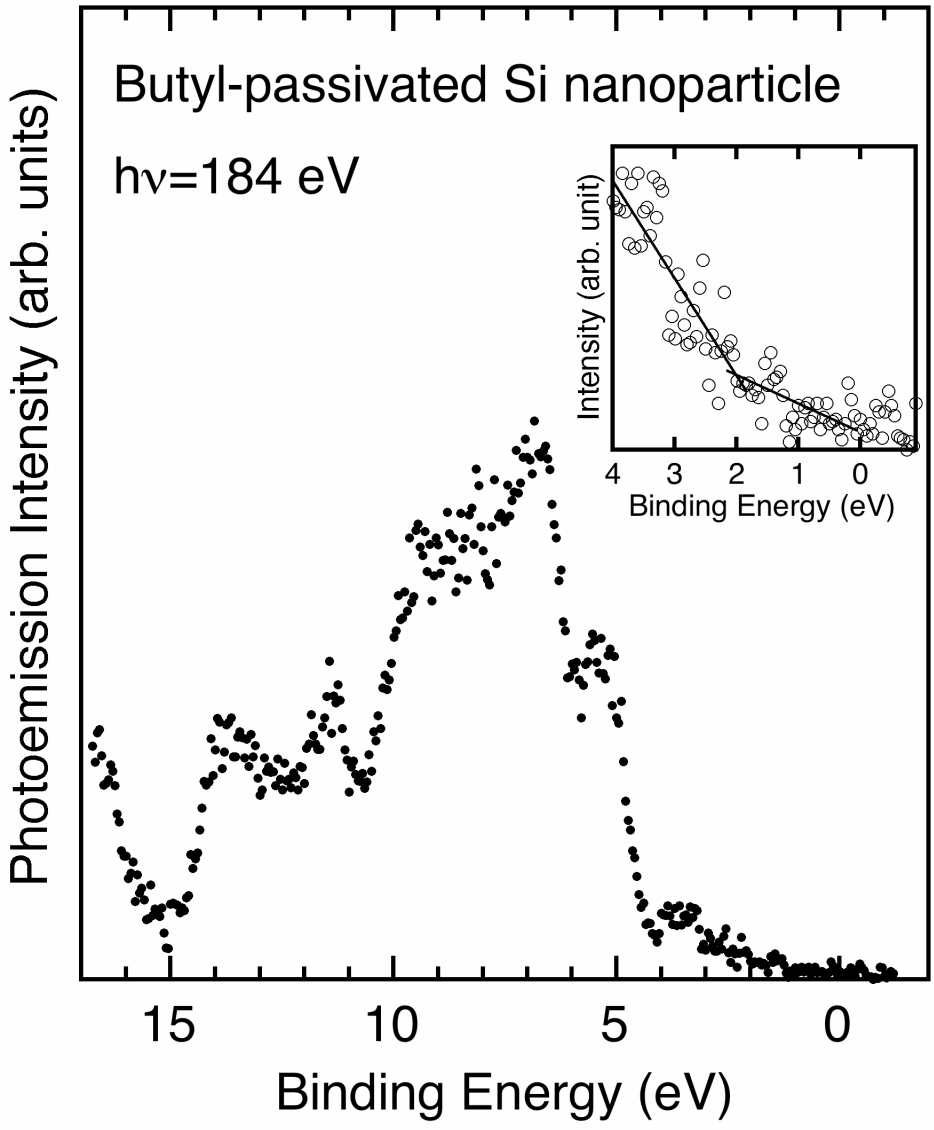

Fig. 3.

A. Tanaka *et al*.